



Pergamon

FUNCTIONALISATION OF GOLD SURFACES VIA TOPOLOGICAL TEMPLATES

Lukas Scheibler[§], Pascal Dumy^{§*}, Dimitris Stamou[#], Claus Duschl[#], Horst Vogel[#] and Manfred Mutter[§]

[§] Institute of Organic Chemistry, University of Lausanne, BCH-Dorigny, CH-1015 Lausanne

[#] Swiss Federal Institute of Technology, EPFL, CH-1015 Lausanne, Switzerland

Received 21 November 1997; accepted 28 January 1998

Abstract : *Regioselectively addressable functionalised templates (RAFT) represent topological cyclic peptides containing orthogonally protected attachment sites pointing to opposite faces of the template backbone. Functionalisation of the template with coordinating groups and alkane chains result in metal-binding and self-association properties in solution without major disruption of the preferred template conformation as inferred by NMR, CD and surface plasmon resonance (SPR) spectroscopy studies. This suggested that the template disposes the appended groups in spatial orientations suitable for their designed functions. Accordingly, a RAFT molecule exhibiting metal-binding sites and thioalkane chains has been incorporated into self-assembled monolayers on gold surfaces and is used to detect external ligand-binding on the surface by SPR spectroscopy. The results demonstrate that RAFT molecules are versatile molecular devices for functionalizing gold surfaces opening a wide range of applications in biosensor technology.* © 1998 Elsevier Science Ltd. All rights reserved.

INTRODUCTION

Great efforts have been devoted to the *de novo* design of peptides and proteins with novel structural and functional properties^{1,2}. In particular, the use of peptide frameworks with defined topology and limited size represents a powerful strategy to embody and direct functional groups such as metal chelating or fluorescent probes in a well defined spatial orientation³. Moreover, an increasing interest in using peptides for the construction of analytical devices to monitor specific recognition reactions between receptors and ligands is observed. Up to date, extensive design is needed for the construction of peptidic scaffolds exhibiting well defined three-dimensional packing topologies⁴. In order to overcome these limitations, we have recently introduced a new type of scaffolds termed Regioselectively addressable functionalised templates (RAFT) containing orthogonally protected attachment sites pointing to opposite faces of the cycle⁵ (Fig. 1). NMR studies supported that these RAFT molecules adopt a well-defined conformation in solution characterised by an antiparallel β-sheet encompassed by two β-turns centred at the Pro-Gly locations⁶. Such RAFT molecules represent a key element in the *de novo* design of proteins using the TASP (Template Assembled Synthetic Proteins) approach⁷ for directing covalently attached secondary structure units into predetermined folding topologies exhibiting tailor-made functional properties⁸.

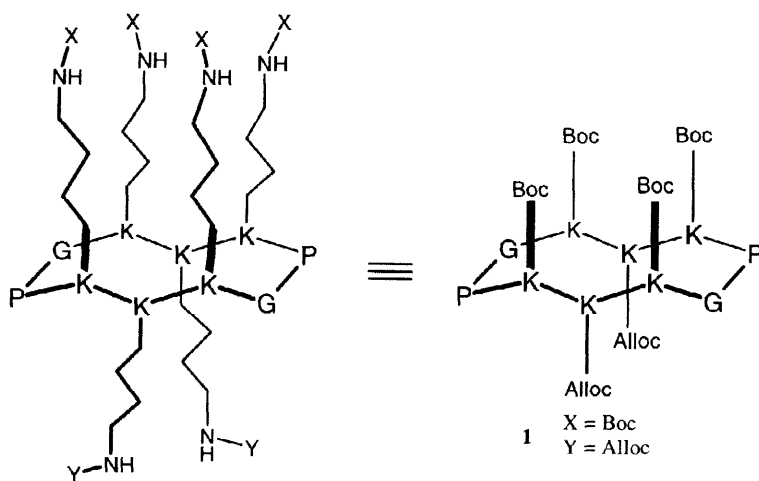


Fig. 1. RAFT molecule (**1**: X=Boc, Y=Alloc) exhibiting two spatially well separated faces. The attachment sites (NH₂ of lysines) are orthogonally protected and thus regioselectively addressable (see Table 1; G = Glycine; P = Proline; K = Lysine; X, Y = ϵ -amino functionalisation of lysine).

More recently, the attachment of various organic molecules and peptides to opposite faces of the template provided a convenient way to modulate the physicochemical properties of the resulting TASP molecules⁹. In this article, we report the synthesis and spectroscopic characterisation of template molecules functionalised with coordinating groups and alkane chains. The resulting molecular systems **1-9** (Table 1) serve as sensing elements on gold surfaces for monitoring the binding of metal ions and external ligands.

RESULTS AND DISCUSSION

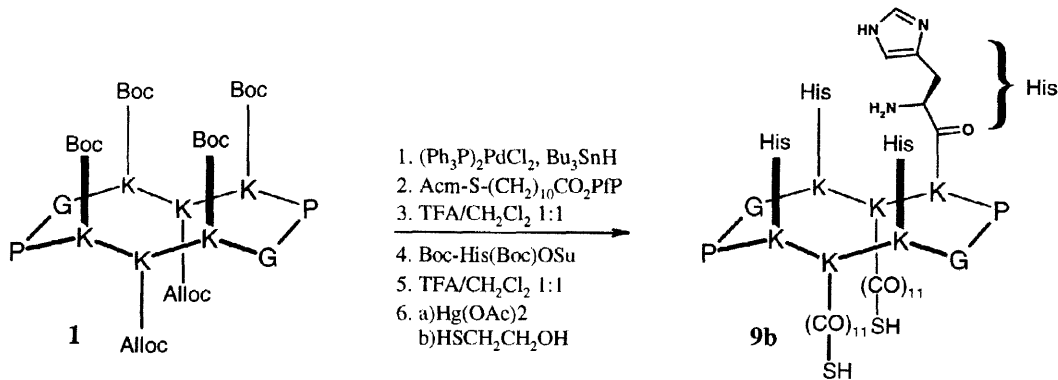
Synthesis. The protected cyclic RAFT molecule **1** (Table 1) was prepared by a combined solid-phase and solution strategy as described previously⁵. A orthogonal strategy based on a combination of Boc and Alloc protecting groups at the lysine side-chains of **1** was used to address selectively the opposite faces (or domains) of the cyclic template.

Table 1: Derivatives of RAFT molecule **1** (Fig. 1)

RAFT compounds	X	Y	Yield (%) ^a
1	Boc	Alloc	
2	H	Alloc	92
3	Fen	Alloc	64
4	His	Alloc	57
5	H	His	74
6	des-amino-His	Alloc	70
7	H	OC-(CH ₂) ₉ -CH ₃	66
8	H	OC-(CH ₂) ₁₀ -SH	42
9a	His	OC-(CH ₂) ₁₀ -S-Acm	86
9b	His	OC-(CH ₂) ₁₀ -SH	37

Fen = 1,10-Phenanthroline-2-carboxylic acid; His = Histidine; Boc = t-Butyloxycarbonyl; Alloc = Allyloxycarbonyl; Acm = Acetamidomethyl. ^a Overall yields after deprotection, coupling and HPLC purification starting from **1**.

Removal of Aloc (Scheme 1, step 1) or Boc (step 3) protecting groups and subsequent acylation with ligands or aliphatic alkane chains afforded derivatives **2–8** (Table 1). For instance, peptides **4** and **5** (Table 1) were obtained by the selective attachment of four respectively two histidines residues after Boc or Aloc removal. Similarly, the synthesis of molecules **9a** and **9b** exhibiting two functional domains is achieved by sequential deprotection-acylation cycles as depicted in Scheme 1.



Scheme 1. Synthesis of RAFT molecule **9b** (see Table 1).

Metal binding properties. Derivatives **2–6** disposing His and Fen groups have been designed to assess and characterise metal binding properties in solution by NMR, CD and UV spectroscopy. The Zinc(II) titration of Fen-containing peptide **3** was monitored by absorption spectroscopy (UV-Vis) as depicted in Figure 2. The $\pi-\pi^*$ transition of the phenanthroline moiety displayed a distinct red shift upon addition of Zn(II) ions (Fig. 2-a). A clean isobestic point was also observed supporting a two-state equilibrium. Therefore, the binding isotherm obtained from variation of absorption at 277 nm (Fig. 2-b) was used to calculate the dissociation constants and ascertain the anticipated template:metal stoichiometry of 1:2¹⁰. The method of continuous variations¹¹ (JOBs-method, Fig. 2, insert) further supported this stoichiometric ratio.

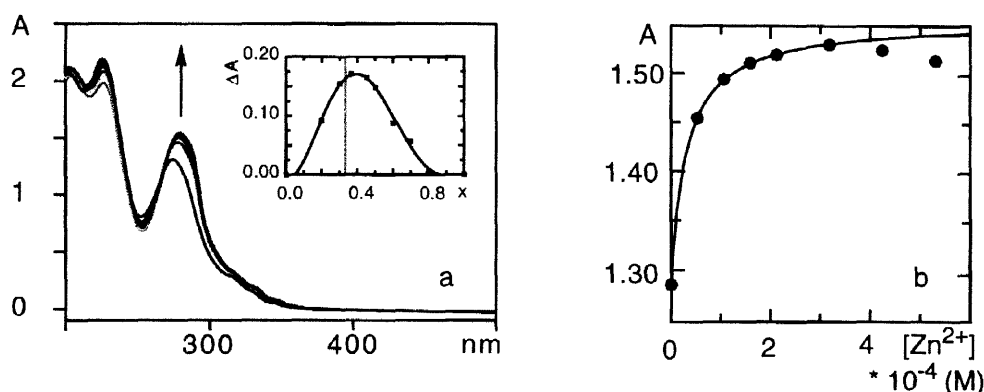


Fig. 2. (a) Absorption spectra of **3** upon addition of $ZnCl_2$ at pH 7.00. Insert: JOB-Plot (x represents the total molar fraction of the template). For a template:metal stoichiometry of 1:2 a theoretical value x_{max} of 0.33 is calculated (found 0.38). (b) Binding isotherm calculated from the change of absorption at 277 nm.

An apparent dissociation constant of $K_d \cdot 10 \mu M$ was obtained for both metal binding sites. Addition of Zn(II) to the His-containing molecules **4** and **5** at neutral pH resulted in a significant increase of peptide

secondary structure as monitored by CD spectroscopy (Fig. 3) and in a specific variation of imidazole ring proton chemical shifts (Fig. 4). The resulting binding isotherms (Fig. 3) provided K_d values of 100 μM and 60 μM for **4** and **5**, respectively¹². Again, a peptide:Zn stoichiometry of 1:2 was found for peptide **4** whereas for **5** a 1:1 ratio was observed in harmony with the number of histidine residues attached.

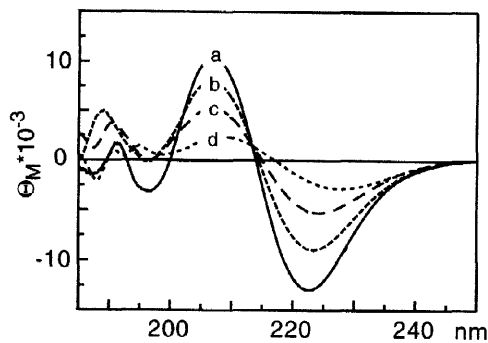


Fig. 3. CD spectra of RAFT **4** as a function of Zn^{2+} complexation in water (pH = 7.0) $[\text{Zn}^{2+}]$ in mM: a = 0; b = 0.19; c = 3.70; d = 37.0.

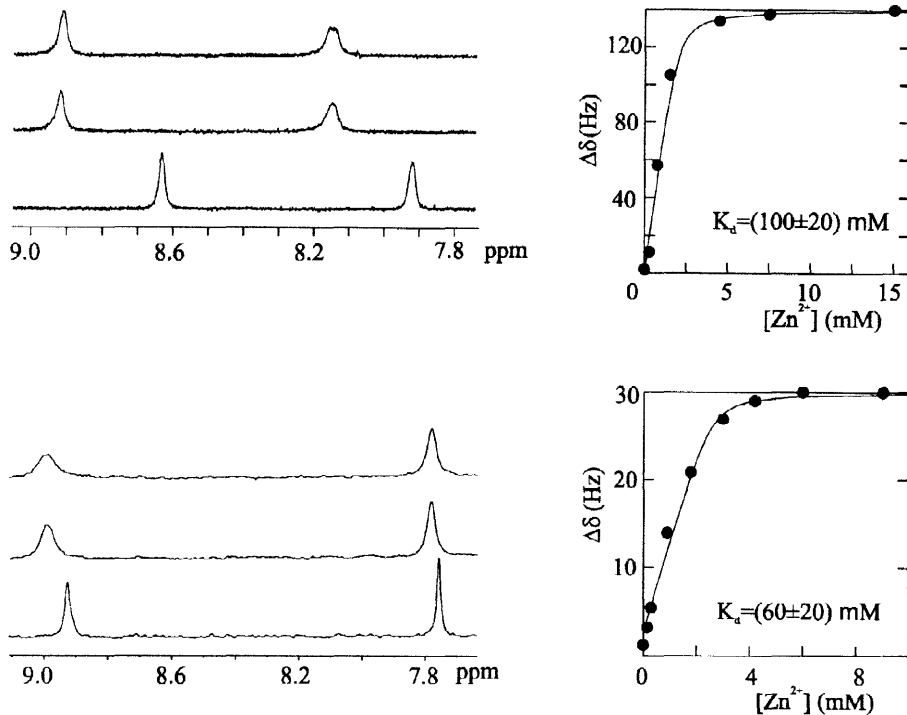


Fig. 4. Variation of the chemical shift of the C-2 and C-4 imidazole protons of RAFT **4** (above) and **5** (below) as function of Zn^{2+} complexation at 400 MHz in $\text{D}_2\text{O}/\text{CD}_3\text{CN}$.

The pH dependent titration of peptides **4** and **5** showed that metal binding is inhibited at pH values below 4.5. For des-aminohistidine-containing peptide **6**, no binding of Zn(II) ions was detected. Furthermore, acylation of the free α -amino groups of the histidine residues suppressed completely the metal-binding properties observed for compound **4** and **5**¹³. Finally, RAFT molecule **2** showed no metal-binding affinities indicating that the metal interaction for compounds **4** and **5** is mediated both by the imidazole ring nitrogens

and the α -amino groups of the histidine residues as coordination ligands as supported by the observed peptide:metal stoichiometry.

Self-assembly properties. Molecule **7–9** bearing hydrophobic aliphatic chains have been prepared for studying micellation and self-assembly in solution. A critical micellar concentration (cmc) of about 0.2 mg.ml^{-1} was measured for compound **7** by surface pressure measurements in aqueous solution (Fig. 5, insert). Therefore, CD spectra have been recorded above and below this cmc value to assess the effect of concentration on the peptide conformation. Above the cmc, a characteristic $n-\pi^*$ minimum at 220 nm and a strong positive $\pi-\pi^*$ at 192–197 nm (Fig. 5, c) close to the theoretically derived class B pattern¹⁴ is obtained. Such CD spectra are consistent with the presence of type II β -turns and β -sheet structures normally observed for RAFT molecules in organic solvents only⁸. Below the cmc, the CD spectrum does not point to the adoption of a particular defined secondary structure (Fig. 5, a). A similar loss of secondary structure was observed in water for the ^6N -deprotected RAFT **2** and rationalised by an increase in the motional flexibility of the cycle^{8,15}. However, upon addition of undecanoic acid, a CD spectrum resembling the one obtained above the cmc is observed (Fig. 5, b).

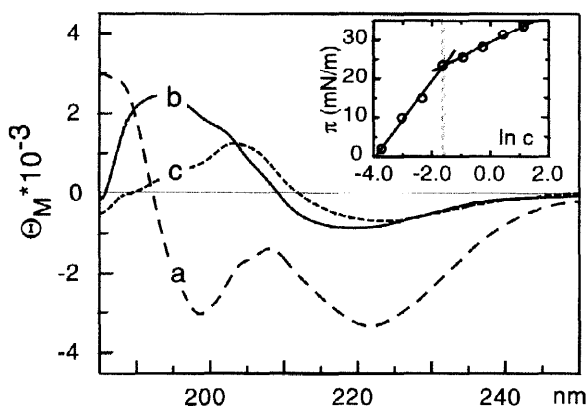


Fig. 5. CD spectra of RAFT **7** in water at concentrations below the cmc (a), after addition of undecanoic acid (b) and above the cmc (c). The insert shows the surface pressure variation as function of the concentration of **7**, representing the critical micellar concentration (cmc) at the line break. a: 0.17 mg/ml ; b: $0.17 \text{ mg/ml} + \text{undecanoic acid}$; c: 1 mg/ml .

These results indicate that hydrophobic interactions promote in water a significant stabilisation of the peptide conformation, presumably upon micelle formation. It is interesting to note that a similar secondary structure stabilising effect can be induced by the addition of Zn(II) to compounds **4** and **5**. Consequently, the chimeric molecule **9a** functionalised with His and hydrocarbon chains, displays a pronounced secondary structure stabilisation upon metal binding as well as upon self-assembly in solution.

Functionalisation of gold surfaces. Terminal thiol groups have been used to address gold surfaces with self-assembled monolayers (SAM) of molecule **8** or **9b** (Fig. 6).

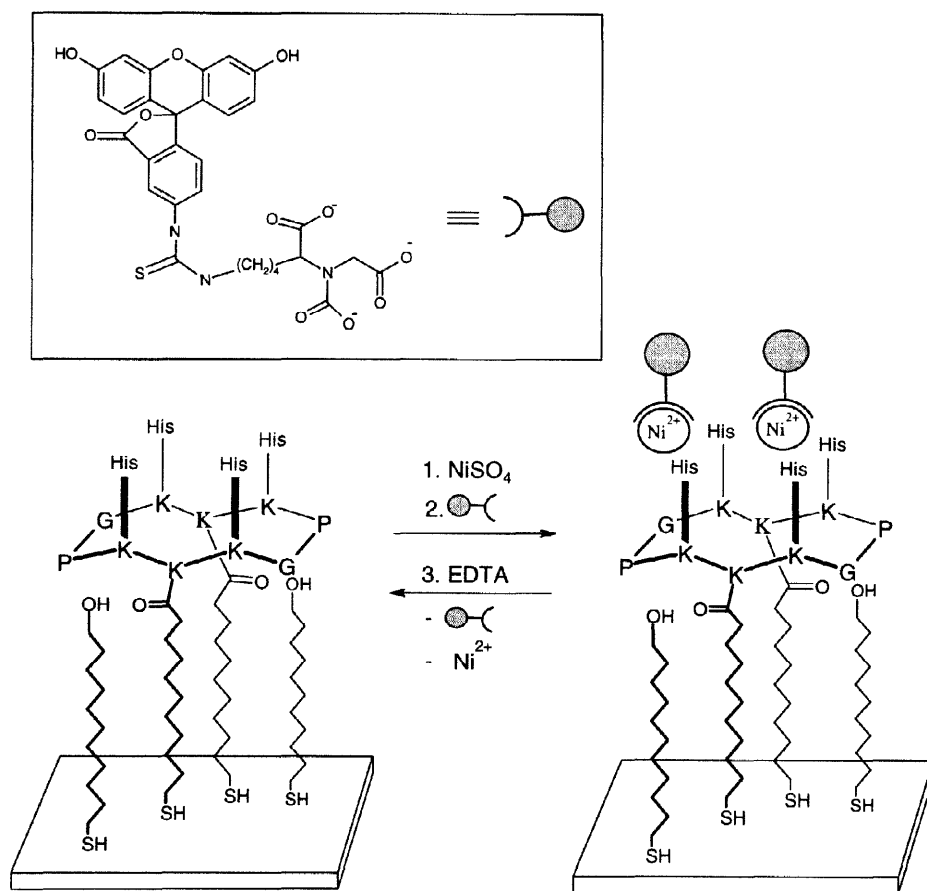


Fig. 6. Schematic representation of RAFT derivative **9b** as self-assembled monolayer (SAM) immobilised on a gold surface showing the reversible binding of NTA labelled fluoresceine ligands (box above). After loading with Ni(II) (step 1), the ligand is bound to the remaining free coordination sites of the coordinated Ni (II) (step 2). Removal of Ni(II) and the ligand is achieved by washing the surface with a EDTA solution (step 3). SPR spectroscopy is used to monitor the interactions of the ligand with the surface by following the distinct change of the resonance angle Θ (Fig. 7).

The self-assembly process on gold was monitored in real time by surface plasmon resonance (SPR) spectroscopy and the remaining accessible surface was subsequently blocked by immobilisation of 11-mercaptoundecan-1-ol. Pure SAM of **8** showed a mass coverage corresponding to a mean area¹⁶ of 150 \AA^2 per molecule whereas a slightly higher value of 180 \AA^2 was determined for **9b**. These values are in good agreement with the NMR derived template geometry⁶. SAM of peptide **8**, disposing free amino groups, provide also a means for further chemical modifications of gold surfaces via RAFT molecules¹⁷. SAM of **9b** disposing histidine residues as metal binding sites, can be considered as an inversion of immobilised metal affinity chromatography¹⁸ (IMAC). After loading of the histidine residues with Ni(II) ions, specific binding of a nitrilotriacetic acid (NTA) derivative¹⁹ to the surface is observed (Fig. 7b). Desorption of this derivative upon addition of EDTA demonstrates the full reversibility of the process (Fig. 6 and 7a). The change of the resonance angle Θ allowed for the estimation of the NTA stoichiometry per template (Fig. 7a). Again, a 1:2 ratio (template : NTA) is found consistent with the results obtained in solution.

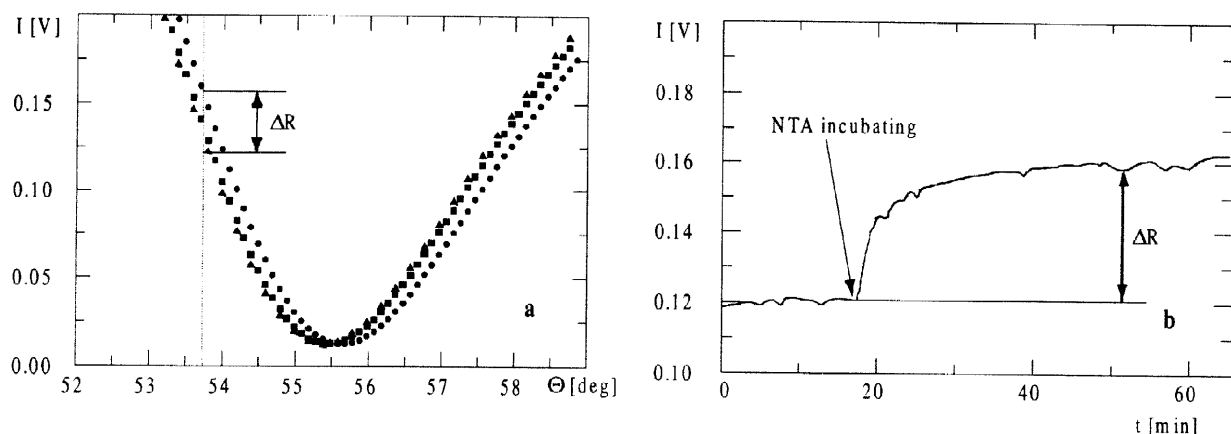


Fig. 7. SPR measurements of surface assembled RAFT **9b** (see Fig. 6). (a) Reflectivity (I) vs. angle (Θ) curves for the mixed SAM of **9b** and 11-mercaptoundecan-1-ol (\blacktriangle), after the complexation of the NTA derivative $\Delta\Theta=0.25^\circ$ (\bullet) and after metal removal with EDTA $\Delta\Theta=0.06^\circ$ (\blacksquare). (b) Time course of the reflected light intensity during the specific binding of the NTA derivative at $\Theta = 53.75^\circ$.

CONCLUSIONS

The regioselective functionalisation of RAFT molecules by hydrocarbon chains, metal chelating groups or combinations thereof is studied to obtain new molecular devices for surface modifications. The flexibility of the synthetic methodology, based on orthogonally protected attachment sites, allows a wide range of combinations of functionalities to be assembled on the bifacial template molecule. The resulting molecular systems exhibit the designed properties such as metal complexation and self-association without disruption of the preferred template conformation. This suggests that the RAFT topology disposes the appended groups in well defined spatial orientations avoiding the extensive design of structurally complex scaffolds. As demonstrated above self-assembly of the bifunctional molecule **9b** on gold surfaces provides a supramolecular array of oriented metal-binding sites. This surface recognises and reversibly binds external ligands. Consequently, the template concept allows for the design of novel molecular systems exhibiting tailored physical and chemical functions, thus offering interesting perspectives in the area of biosensor- and nano-technologies.

EXPERIMENTAL

Materials and Methods. Solid phase peptide synthesis was done on a semi-automatic Advanced ChemTech ACT200 Peptide Synthesiser. HPLC was performed on Waters equipment using columns packed with Vydac Nucleosil 300Å 5 μm C18 particles unless otherwise stated. Solvent A consisted of 0.09% TFA and solvent B of 0.09% TFA in 90% acetonitrile unless. Amino-acid analyses were performed on a Perkin-Elmer HPLC. Mass spectra were obtained by electron spray ionisation (ESI-MS) on a Finnigan MAT SSQ 710C. Circular dichroism (CD) spectra were recorded at room temperature on a Jobin Yvon CD Mark V spectropolarimeter using quartz cells of 0.1 mm path length. The instrument was calibrated with D-10-camphorsulphonic acid. ^1H NMR spectra were obtained on a Bruker DPX-400. UV/VIS spectra were obtained on a computerised Perkin Elmer Lambda 7 using 1 cm cells.

$c\{HN\text{-}K(Boc)\text{-}P\text{-}G\text{-}K(Boc)\text{-}K(Aloc)\text{-}P\text{-}G\text{-}K(Boc)\text{-}K(Aloc)\}$ (**1**) = $T(Boc)_4(Aloc)_2$. **1** was prepared following published procedure⁵, 780 mg, (76%), $t_R = 24.6$ min (gradient 25% B to 100% B in 30 min), $R_f = 0.35$ (CHCl₃ / MeOH = 9 / 1), ESI-MS: 823.8 ((M+2H)/2), m.p. > 250°C, ASA: G 1.74 (2), K 6.0 (6), P 1.83 (2)

$T(NH_2)_4(Aloc)_2$ (**2**). The protected template **1** (50 mg, 30 μmol) was dissolved in 10 ml of 50% TFA solution in DCM for 45 min. After removal of the solvent under reduced pressure, the residue was precipitated with diethyl ether and

lyophilised. Yield: 47 mg (92%), $t_R = 18.6$ min (gradient 25% B to 100% B in 30 min), ESI-MS: 416.8 ((M+3H)/3), 454.0 ((M+TFA+2H)/3), 623.8 ((M+2H)/2), 680.6 ((M+TFA+H)/2), 737.8 ((M+2TFA)/2)

T(Fen)4(Aloc)2 (3). The 1,10-phenanthroline-2-carboxylic acid (Fen) was synthesised according the protocol of Corey et al²⁰. A solution of T(NH₂)₄(Aloc)₂ (2) (47 mg, 37 μ mol), Fen (50 mg, 230 μ mol), HATU²¹ (90 mg, 230 μ mol) in of dry DMF (10 ml) was treated with DIEA (70 μ l, 720 μ mol) for 3h. The solvent was removed and the crude residue precipitated with diethyl ether and then purified by RP-HPLC. Yield: 50 mg (64%), $t_R = 19.25$ (gradient 5% B to 100% B in 38 min) ESI-MS: 518.8 ((M+4H)/4), 691.5 ((M+3H)/3), 1026.4 ((M+2H)/2).

T(His)4(Aloc)2 (4). A solution of T(NH₂)₄(Aloc)₂ (2) (20 mg, 12 μ mol), N α -Boc-His(Boc)-OSu (22 mg, 48 μ mol) in dry DMF (2 ml) was treated with DIEA (35 μ l, 96 μ mol) at room temperature. The reaction was complete after 3 h and after removal of the volatile the residue was treated with a 50% solution of TFA in DCM during 45 min. The solvent was evaporated and the remaining residue was purified by preparative RP-HPLC to yield 12 mg (57%) of pure product. $t_R = 18.59$ min (gradient 0% B to 100% B in 40 min), ESI-MS: 898.1 ((M+2H)/2), ASA: G 1.82 (2), H 4.83 (4), K 6.12 (6), P 2.02 (2)

T(NH₂)₄(His)2 (5). A solution of the protected template **1** (100 mg, 61 μ mol), 1.6 ml glacial acetic acid, PdCl₂(PPh₃)₂ (1-3 mg) in 40 ml DCM was treated with Bu₃SnH (100 μ l, 150 mmol) added in two portion. When the reaction was complete (1h, HPLC), the orange solution was concentrated and the crude brown residue was dissolved in MeOH and precipitated with diethyl ether. The solid was dissolved in water, filtered through Celite and then lyophilised to afford 81 mg (83%) of the product. $t_R = 18.3$ min (gradient 25% B to 100% B in 30 min), ESI-MS: 739 ((M+2H)/2). A mixture of the Aloc deprotected template (10 mg, 6.7 μ mol), N α -Boc-His(Boc).OSu (6.5 mg, 41.2 μ mol) in dry DMF (2 ml) was treated with DIEA (10 μ l, 55 μ mol). After 2 h the reaction was complete as inferred by HPLC, the solvent was removed and the residue was deprotected with 2 ml of a 50% solution of TFA in DCM for 30 min. The solvent was removed and the residue was purified on a Waters Sep-Pak Vac 35cc (2g) Cartridge using 10% B in water as eluent. Lyophilisation afforded 6.8 mg (74%) of the desired product. $t_R = 10.35$ min (gradient 5% B to 100% B in 38 min) ESI-MS: 451.3 ((M+3H)/3), 489.3 ((M+TFA+2H)/3), 676.3 ((M+2H)/2), 733.6 ((M+TFA+H)/2)

T(des-aminoHis)4(Aloc)2 (6). A solution of T(NH₂)₄(Aloc)₂ (2) (10 mg, 5.8 μ mol), des-aminohistidine (Bachem, CH) (5 mg, 32 μ mol), PyAOP (17 mg, 32 μ mol) in dry DMF (2 ml) was treated with DIEA (20 μ l, 128 μ mol) for 4 h. The solvent was removed and the residue purified by RP-HPLC to yield 7 mg (70%) of **6**. $t_R = 19.53$ min (gradient 0% B to 100% B in 40 min), ESI-MS: 434.9 ((M+4H)/4), 579.1 ((M+3H)/3), 868.0 ((M+2H)/2), 1735.0 (M+H).

T(NH₂)₄(OC-(CH₂)₉-CH₃)₂ (7). A solution of undecanoic acid (2.00 g, 10.7 mmol), pentafluorophenol (2.20 g 12 mmol) in dry DCM (5 ml) was treated with dicyclohexylcarbodiimide (DCC) (2.44g 12 mmol). After 1h, the solution was filtered, the volatile removed under vacuum and the residue purified by chromatography column with petrolether / diethyl ether (9:1) to afford an 3.55g of an oil (94%). Aloc groups were removed of **1** following the protocol described for **5**. A solution of this deprotected peptide (30 mg, 20 mmol), undecanoic-pentafluorophenyl ester (7.2 mg, 40 mmol) and 4-dimethylaminopyridine (DMAP) in DMF (2 ml) was treated with DIEA (15 ml, 80 mmol) for 12h. After removal of the solvent and precipitation with diethyl ether, the residue was deprotected with a solution of 50%TFA in DCM during 45 min. Evaporation and RP-HPLC purification afforded 19 mg (66%) of **7**. $t_R = 20.43$ min (gradient 25% B to 100% B in 30 min), ESI-MS: 472.6 ((M+3H)/3), 510.8 ((M+2H+TFA)/3), 707.7 ((M+2H)/2), 765.0 ((M+H+TFA)/2), 114.6 (M+H).

T(NH₂)₄(OC-(CH₂)₁₀-SH)₂ (8). Acm-S-11-mercaptopoundecanoic acid, 11-mercpto-undecanoic acid (1.00 g, 4.58 mmol) and acetamidomethanol (409 mg, 4.58 mmol) were dissolved in 50 ml trifluoroacetic acid and stirred for 30 min at room temperature. After solvent removal the residue was dissolved in CHCl₃ and extracted with 2N NaOH. The aqueous phases were acidified and extracted with CHCl₃. The organic layer was dried over MgSO₄ and the solvent removed under pressure. The product was crystallized with DCM / petrol ether to afford 950 mg (72%) of pure **8**. $R_f = 0.26$ (diethyl ether / acetic acid = 98 : 2), m.p. 81°C, $t_R = 17.19$ (gradient 25% B to 100% B in 30 min), ESI-MS: 290.5 (M+1), 312.4 (M+Na), ¹H-NMR: 1.15 (m, 12H, H alkane chain), 1.27 (m, 6H, H alkane chain), 1.95 (s, 3H, CH₃CO), 2.30 (td, 2H, S-CH₂- alkane chain), 4.30 (d, 2H, N-CH₂-S), 4.6 (s, large, 1H, acid), 5.75 (s, large, 1H, NH).

Acm-S-11-mercaptopoundecanoic-pentafluorophenyl ester: Acm-S-11-mercaptopoundecanoic acid (100 mg, 346 mmol), pentafluorophenol (70 mg, 380 mmol) and DCC (206 mg, 380 mmol) were reacted in CHCl₃ (4 ml). The solution was filtered after 12 h, extracted with a solution of 5% KHSO₄, 10% NaHCO₃ and NaCl_{sat} and the organic phase dried over MgSO₄. After removal of the solvent 99 mg (63%) of the desired active ester was obtained. $R_f = 0.7$ (diethyl ether/acetic

acid = 98 : 2), m.p. 67–68°C, t_R = 17.59 (gradient 25% B to 100% B in 30 min), ESI-MS: 456.7 (M+1), $^1\text{H-NMR}$: 1.15 (m, 12H, H alkane chain), 1.22 (m, 6H, H alkane chain), 1.95 (s, 3H, CH_3CO), 2.30 (td, 2H, S- CH_2 - alkane chain), 4.30 (d, 2H, N- $\text{CH}_2\text{-S}$), 5.75 (s, large, 1H, NH).

T(Boc)4(OC-(CH₂)₁₀-S-Acm)2: The Aloc groups were removed according the procedure described for **5**. A solution of the deprotected template (40 mg, 27 μmol), Acm-S-11-mercaptoundecanoic-acidpentafluorophenolester (25 mg, 55 μmol), DMAP in dry DMF was treated with DIEA (100 μl , 580 μmol). The solvent was removed after 9 h and the residue precipitated with diethyl ether to afford 50 mg (91%) of the product. t_R = 24.82 min (gradient 25% B to 100% B in 30 min), ESI-MS: 1010.6 ((M+2H)/2).

T(NH₂)₄(OC(CH₂)₁₀SAcm)2: T(Boc)4(OC(CH₂)₁₀SAcm)2 (50mg, 25 mmol) was treated according the protocol used for **2**. Yield: 41.8 mg (81%), t_R = 13.99 min, ESI-MS: 810.7 ((M+2H)/2)

T(NH₂)₄(OC-(CH₂)₁₀-SH)2 (8): T(NH₂)₄(OC(CH₂)₁₀SAcm)2 (50 mg, 24 μmol) and Hg(OAc)₂ (20 mg, 50 μmol) were stirred for 2h in 5 ml 30% acetic acid under N₂ atmosphere. β -Mercaptoethanol (430 μl , 4.8 mmol) was added and the solution stirred overnight. The solution was filtered and purified by preparative RP-HPLC to afford 29 mg (62%) of pure **8**. t_R = 18.61 min (gradient 25% B to 100% B in 30 min), ESI-MS: 493.3 ((M+3H)/3), 531.2 ((M+3H+TFA)/3), 739.8 ((M+2H)/2), 796.8 ((M+2H+TFA)/2), 797.2 ((M+2TFA)/2), 1478 (M+1).

T(His)₄(OC-(CH₂)₁₀-S-Acm)2 (9a): T(NH₂)₄(OC(CH₂)₁₀SAcm)2 (73 mg, 49 μmol) was prepared according the protocol for **8** and then treated following the protocol for **4** to afford 100 mg (86%) of product. t_R = 12.55 min (gradient 0% B to 100% B in 40 min), ESI-MS: 542.9 ((M+4H)/4), 724.2 ((M+3H)/3), 1084 ((M+2H)/2).

T(His)₄(OC-(CH₂)₁₀-SH)2 (9b): T(His)₄(OC(CH₂)₁₀SAcm)2 (20 mg, 9.2 μmol) was treated according to the protocol for **8** affording 12 mg (64%) of product. t_R = 16.65 min (gradient 0% B to 100% B in 40 min), ESI-MS: 507.0 (M/4+1), 676.6 ((M+3H)/3), 1014.2 ((M+2H)/2).

Surface plasmon resonance (SPR). The surface plasmon resonance measurements were performed, using the Kretschmann coupling scheme²² on a home-made computerised reflection apparatus as described in details elsewhere²³. At the resonance angle the incident laser beam (He-Ne laser, 632.8 nm, p-polarised) couples via an equilateral, high index prism (SF 10, $n=1.723$) to the surface plasmon mode in a thin gold film (40 nm).

Layer formation. For the self-assembly of peptide and 11-mercaptoundecanol, a gold film (40 nm), vacuum evaporated on a cleaned glass slide, was incubated in peptide or thiol water/methanol mixtures. After 1h self-assembly, the surface was extensively washed with water/methanol. Finally a solution of thioalcohols in methanol/water was added to block remaining defects in the monolayer. The binding was monitored *in situ* using surface plasmon resonance. For Ni²⁺ binding the surface was incubated with 100 mM NiSO₄ solution for 10 min. After washing, the cell was calibrated with buffer and the fluoresceine-labelled NTA was added. The surface was washed with buffer and the final thickness measured. The His-exposing surface was regenerated by washing with 0.5 M EDTA in buffer.

UV/VIS Measurements of (Fen)4-Temp-(Aloc)2 (3). A $2.665 \cdot 10^{-5}$ M solution in 10 mM Tris/HCl buffer pH = 7.0 of the decapeptide **3** was titrated in a 1 cm cell with a $5.31 \cdot 10^{-3}$ M solution of Zn(BF₄)₂ at room temperature. The reference cell contained the buffer and the equivalent amount of metal. Job-Plot measurements were obtained by mixing a peptide and a metal solution (both $5.31 \cdot 10^{-5}$ M in buffer) in various ratios affording always the same amount of final solution (1 ml). The reference cell contained the same concentration of peptide in buffer. In this manner a difference spectra between ligated and free peptide was obtained. Job-Plot data points were recorded at $\lambda = 277$ nm.

CD Titrations. CD spectra were obtained in a 1 mm cell with a peptide solution of about 0.5 mg.ml⁻¹ in a Tris / HCl buffer pH 7.0 and titrated with a 100 times more concentrated ZnCl₂ solution in the same buffer. Exact peptide concentration was determined by quantitative ASA. For each spectra 2 scans were accumulated, the resolution was set to 0.2 nm and the integration time to 2s per step.

NMR Titrations. NMR spectra were measured in acetonitrile CD₃CN / D₂O (1:1), pH being adjusted with NaOD solution to a value of pH = 7. Peptide concentration was 20 mg.ml⁻¹ and the titration was performed with addition of concentrated ZnCl₂ solution.

Surface pressure. Surface pressure was measured a Langmuir balance. Peptide **7** (6.2 mg) was dissolved in pure water (2 ml) in a Teflon cell. The sample was then successively diluted and the corresponding surface pressure was determined after the sample reached equilibrium (constant pressure over more than 5 min). This took normally about 20 min.

Acknowledgements: This work was supported by the Priority Program Biotechnology of the Swiss National Science Foundation.

REFERENCES AND NOTES

* To whom the correspondance should be addressed, e-mail pascal.dumy@ico.unil.ch.

1. Tuchscherer, G.; Mutter, M. *Chem. & Ind.* **1997**, 597-601. Regan, L. *Trends Biochem. Sci.* **1995**, 20, 280-285 and references cited therein.
2. Ackerfeldt, K. S.; Lear, J. D.; Wasserman, Z.R.; Chung, L.A.; DeGrado, W. F. *Acc. Chem. Res.* **1993**, 26, 191-197. Rabanal, F.; DeGrado, W. F.; Dutton, P. L. *J. Am. Chem. Soc.* **1996**, 118, 473-474.
3. Voyer, N.; Lamothe, J. *Tetrahedron*, **1995**, 51, 9241-9244. Cheng, R.P.; Fisher, L.S.; Imperiali, B. *J. Am. Chem. Soc.* **1996**, 118, 11349-11356. Struthers, M.D.; Cheng, R.P.; Imperiali, B. *J. Am. Chem. Soc.*, **1996**, 118, 3073-3081. Mihara, H.; Tanaka, Y.; Fujimoto, T.; Nishino, N. *J. Chem. Soc. Perkin Trans. 2* **1995**, 1915-1921. Mihara, H.; Tanaka, Y.; Fujimoto, T.; Nishino, N. *J. Chem. Soc. Perkin Trans. 2* **1995**, 1133-1140.
4. Schneider, J. P.; Kelly, J. W. *Chem. Rev.*, **1995**, 95, 2169-2187. And references cited therein.
5. Dumy, P.; Eggleston I.; Cervigni, S.; Sila, U; Sun, X.; Mutter, M. *Tetrahedron Lett.* **1995**, 36, 1255-1258
6. Dumy, P.; Eggleston I.-M., Esposito G.; S. Nicula, Mutter, M. *Biopolymers*. **1996**, 39, 297-308.
7. Mutter, M.; Vuilleumier, S. *Angew. Chem. Int. Ed. Engl.*, **1989**, 28, 535-554.
8. Tuchscherer, G.; Servis, C.; Corradin, G.; Blum, U.; Mutter, M. *Proteins Sci.* **1992**, 1, 1377-1386. Pawlak, M.; Meseth, U.; Dhanapal, B.; Mutter, M.; Vogel, H. *Protein Sci.* **1994**, 3, 1788-1805. Mutter, M.; Dumy, P.; Garrouste, P.; Lehmann, C.; Mathieu, M.; Peggion, C.; Peluso, S.; Razaname, A.; Tuchscherer, G. *Angew. Chem. Int. Ed. Engl.* **1996**, 35, 1482-1485.
9. Dumy, P.; Scheibler, L.; Cervigni, S.; Vogel, H.; Mutter, M. *Peptides 1996; Chemistry and Biology 24th Proc. Eur. Pept. Symp.* **1997**, Eds Ramage, H., ESCOM, Leiden, in press.
10. The K_d values were calculated as follows (shown for NMR-titrations):

$$K_d = \frac{[T][M]}{[C]}; [C] = [M_0] - [M]; [T] = [T_0] - [C] \text{ with } [T] = \text{template}, [M] = \text{metal}, [C] = \text{complex}$$

$$\text{For } [T] = -\alpha \cdot \Delta F(\text{Hz}); \Delta F = \text{chemicalshift in Hz, one obtains } [M_0] = -\alpha \cdot \Delta F(\text{Hz}) + ([T_0] - K_d) + \frac{K_d \cdot [T_0]}{\alpha \cdot \Delta F(\text{Hz})}$$

This formula allows the fitting of ΔF against $[M_0]$ and the determination of K_d and $[T_0]$. A $[T_0]$ concentration twice the actual weight in concentration was obtained, indicating that two metal ions were bound independently per RAFT molecule **4**.

11. The maximal change in absorption was found to be at a total molar fraction of the template $x=0.38$. The theoretical value of $x=0.33$ for a template to metal complex of 1:2 is within the error limits.
12. For the calculation of K_d values, only the histidine C₄ proton chemical shift was considered.
13. Acetylation of the RAFT **4** was performed with O-carboxymethylhydroxylamine.
14. Woody, R. W. In *The Peptides 7*, **1985**, Hruby, V.J., Ed., Academic Press, New York, pp. 15-114.
15. Dumy, P.; Eggleston I.-M.; Esposito G.; Nicula, S.; Mutter, M. *Electronic Conference on Trends in Organic Chemistry, (ECTOC-1)*, Rzepa, H., Goodman, J. M. (Eds), (CDROM), Royal Society of Chemistry Publications, **1995**, See also <http://www.ch.ic.ac.uk/ectoc/>.
16. For determination of the thickness and the mass loading, a refractive index $n=1.45$, a refractive index increment $dn/dc = 0.18 \text{ cm}^3 \text{ g}^{-1}$ and a typical peptide density of $\rho = 1.37 \text{ g cm}^{-3}$ was used.
17. The chemical modification with peptides will be reported in due time.
18. Porath, J.; Carlsson, J.; Olsson, I.; Belfrage, G. *Nature* **1975**, 258, 598.
19. We thank A. Heusler (EPFL) for the synthesis of the NTA derivative.
20. Corey, E.J.; Borror A.L.; Foglia, T. *J. Org. Chem.*, **1965**, 30, 288-290.
21. Carpino, L.A.; El-Faham, A.; Minor, C.A.; Albericio, F. *J. Chem. Soc., Chem. Com.* **1994**, 201-203.
22. Kretschmann, E. *Optics Communications* **1972**; 6, 185-186.
23. Terrettaz, S.; Stora, T.; Duschl, C.; Vogel, H. *Langmuir* **1993**, 9, 1361-1369.